RUN 2 COLLIMATION OVERVIEW

N. Fuster Martinez[1], A. Abramov[1,4], G. Azzopardi[1,3], E. Belli[1], C. Boscolo-Meneguolo[1], R. Bruce[1], M. D'Andrea[1,6], M. Di Castro[1], M. Fiascari[1], A. Fomin[1,5], H. Garcia-Morales[1,4], A. Gorzawski[1,3] P. D. Hermes[1], R. Kwee-Hinzmann[1,4], D. Kodjaandreev[1], A. Mereghetti[1], D. Mirarchi[1, 2], J. Molson[1], L. Nevay[1,4], M. Patecki[1], E. Quaranta[1], S. Redaelli[1], A. Rossi[1], R. Rossi[1], B. Salvachua[1], M. Solfaroli Camillocci[1], G. Valentino[1,3], A. Valloni[1], J. Wagner[1].
[1] CERN, Geneva, Switzerland, [2] Manchester University, Manchester, UK,
[3] University of Malta, Msida MSD2080, Malta, [4] Royal Holloway University of London, UK,
[5] NSC Kharkiv Institute of Physics and Technology, Kharkiv, Ukraine,
[6] Università degli Studi di Padova, Padova, Italy.

Abstract

The LHC collimation system is designed to provide protection against regular and abnormal losses in order to reduce the risk of quenches of the superconducting magnets as well as the background in the experiments. All Run 2 proton and ion runs were successfully completed with no magnet quenches from slow losses of the circulating beam. The present contribution reviews the performance of the collimation system in the 2018 run and gives an overview of the performance during Run 2. This paper presents the cleaning performance for protons and ions and the collimation system availability. In addition, the improvements and experience gained with the collimator controls and with the new collimation hardware are discussed, together with the performance of the collimation system during the special high-β^* physics runs. Finally, the new hardware to be installed during LS2 is described and the operational implications discussed.

INTRODUCTION

The Large Hadron Collider (LHC) [1] is equipped with a multi-stage collimation system [2–6] that is designed to handle the normal and the abnormal beam losses in order to minimise the risk of quenches of the superconducting (SC) magnets as well as to reduce the background in the experimental regions. The LHC has two main collimation insertions: the betatron cleaning insertion in Interaction Region 7 (IR7) and the off-momentum cleaning insertion in IR3. The LHC multi-stage collimation system is organised in a well-defined transverse hierarchy with different collimator families. The preservation of the hierarchy between families is a pre-requisite to ensure a good performance of the system. In IR3 and IR7, the first collimators seen by the beam are the primary collimators (TCPs). The TCP jaws are made of Carbon Fiber Composite (CFC) and they are the closest collimators to the beam. The secondary collimators (TCSGs), also made of CFC, and the absorbers (TCLAs) are placed to absorb particles out-scattered by the TCPs. The tertiary collimators (TCTs) are installed close to the Interaction Points (IPs) of the experiments in IP1/2/5/8. They are made of Inermet-180 (heavy Tungsten-alloy) and they aim to absorb the tertiary betatron beam halo. In addition, two collimators per beam (TCSP, TCDQ) are installed in IR6 for dump protection and are made of CFC. These collimators must ensure the protection of the machine in case of asynchronous beam dump (ABD) failures. During the Long Shutdown 1 (LS1), a total of 32 new collimators were installed to improve the Run 1 (2010-2012) collimation system towards higher beam energies and intensities; these included 18 new collimators with embedded Beam Position Monitors (BPMs) (16 TCTPs and 2 TCSPs), additional physics debris collimators (TCLs) with jaws made of Cu, passive absorbers and the re-installation or displacement of existing collimators [7].

During Run 2 (2015-2018), the LHC collimation system provided an excellent performance for all machine configurations including the luminosity levelling methods implemented in 2017 and 2018 accommodating the experiment requirements. Energies of stored proton beams above 300 MJ were reached in 2017 and 2018 (see Fig. 1a). No magnet quenches were recorded from slow circulating beam losses. The good performance of the collimation system was a crucial ingredient to achieve this result, as well as the good orbit stability and beam lifetime achieved [8].

The stored energies reached with Pb ion beams in Run 2 are also shown in Fig. 1b. Also with ion beams no magnet quenches were recorded due to slow losses from circulating beams. However, in the 2018 run in which higher stored energies were achieved, 7 out of 48 fills were dumped by high losses in IR7 [9] caused by periodic orbit oscillations with a frequency of around 10 Hz. The observed worsening by two orders of magnitude of the cleaning inefficiency for ions with respect to that of protons [10] made the ion operation more difficult and limits the current maximum intensity reach.

In this paper, the performance and experience of the collimation system in the 2018 run and in Run 2 is reviewed. In the first section the evolution of the collimator settings in Run 2 as well as those deployed in 2018 runs are briefly described. In the second section, the cleaning performance for protons and ions is presented, followed by the collimation-system availability in the third section. In addition, the improvements and the experience gained with the collimator controls and with the new collimation hardware are presented in the fourth and fifth sections, respectively. The performance of the collimation system was also crucial during the special runs. In 2018, the implementation of two novel collimation

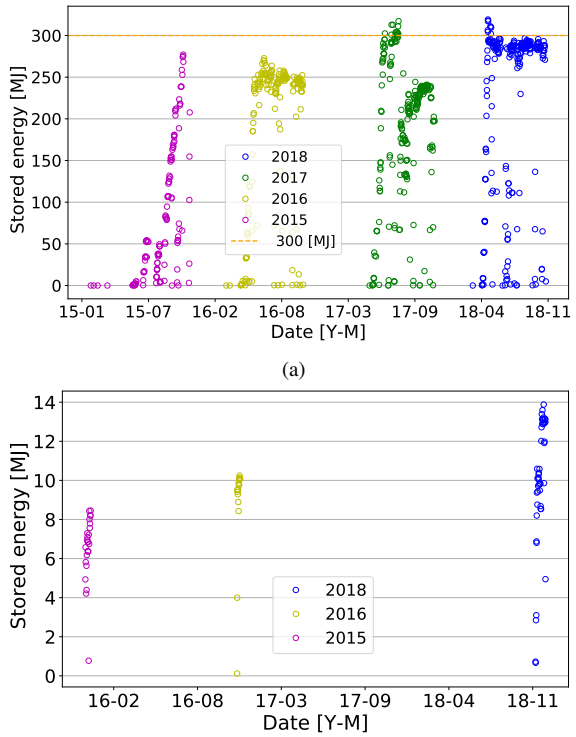

Figure 1: Overview of total stored beam energy in Run 2 for Beam 1 during proton (a) and Pb ion (b) runs.

schemes were crucial during the special high-β^* physics run. The main results are described in the sixth section of this paper. Finally, in the last section the new hardware to be installed during LS2 is presented and the operational implications are discussed.

EVOLUTION OF COLLIMATOR SETTINGS

The choice of the collimator settings is a compromise between the smallest protected machine aperture determining β^* [11], the background in the detectors, and the TCP cut that aims to clean the beam halo without introducing intolerable levels of impedance (mainly induced by TCPs and TCSGs). In addition, all the families must fit in between the primary cut and the smallest protected aperture with margins to take into account beam operational errors such as beam offset, machine imperfections, etc.

All along Run 2, the β^*-function in the experiments has been decreased in order to increase luminosity. In the 2018 proton run, the collimation system had to accommodate in ATLAS and CMS, a β^*-function of 25 cm at the end of the β^*-levelling. The margins between the TCTs and the TCSPs had to be squeezed to unprecedented levels. This was possible thanks to the experience gained during Run 2 on the control of the MKDs-TCTs phase advance [11], the better knowledge on the real aperture bottleneck [12] and of the beam orbit monitoring performed at the TCTs with the embedded BPMs that were installed during LS1. For each collimator family, in Fig. 2a the smallest collimator setting in units of beam σ is shown for the proton runs. In 2018, the same collimator settings in mm as in 2017 were used for all the families, however as the β^*-function in ATLAS and CMS was squeezed down from 30 to 25 cm a difference is observed for the tertiary collimators (see Fig. 2a green and red lines).

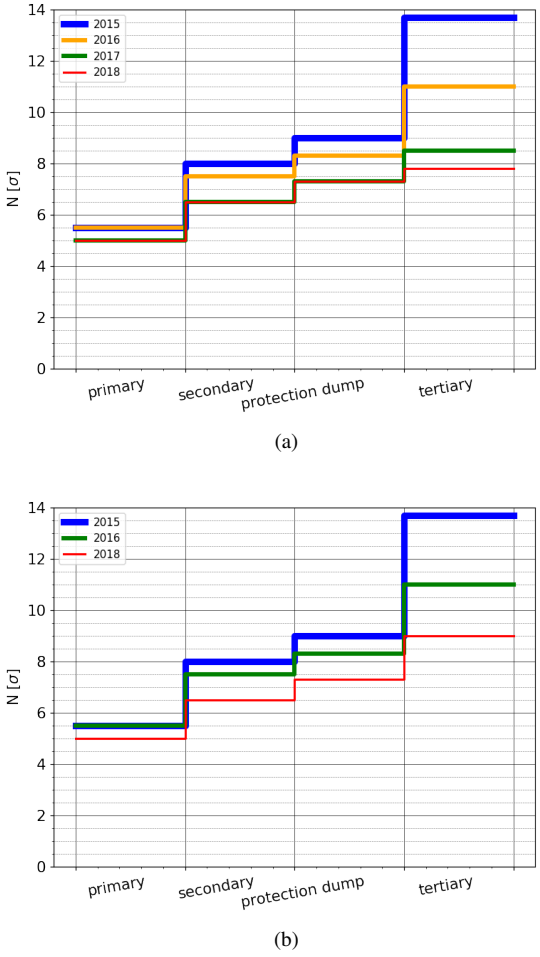

Figure 2: Overview of the collimator settings, for a normalised emittance of ϵ_N=3.5 μm, for the cleaning hierarchy in IR7, the dump protection in IR6, and the TCTs in IR1 and IR5 during Run 2 for protons (a) and ions (b). For the proton 2018 TCTs settings only the last point of the β^*-levelling is plotted.

The deployed collimator settings in the 2018 proton runs are shown in more detail in Table 1 for the different points in the cycle (injection, Flat Top (FT) and physics for different values of the β^*-function), in which β^*-functions in ATLAS and CMS are indicated. Notice that due to the use of the Achromatic Telescopic Squeeze (ATS) [13] optics and the fact that the TCDQ can not be moved at top energy due to interlock constraints, the effective sigma setting varies in IR6 as the β^*-function changes in the squeeze differently for the two beams. In addition, the settings for the TCLs, for

Table 1: Collimator settings of the 2018 standard operation proton run for a normalised emittance of ϵ_N=3.5 μm.

Collimator	**Beam**	**IR**	**Injection β^*=1 m**	**FT β^*=30 cm**	**Physics β^*=27 cm**	**Physics β^*=25 cm**	**Physics**
TCPs/TCSGs/TCLAs	B1/2	7	5.7/6.7/10	5/6.5/10	5/6.5/10	5/6.5/10	5/6.5/10
TCPs/TCSGs/TCLAs	B1/2	3	8/9.3/10	15/18/20	15/18/20	15/18/20	15/18/20
TCTs	B1/2	1/5	13	15.0	8.5	8.1	7.8
TCDQ / TCSP	B1	6	8/7	7.88	7.42	7.34	7.30
TCDQ / TCSP	B2	6	8/7	7.36	7.24	7.28	7.30
TCL.4	B1/2	1/5	out	out	16.4	15.6	15
TCL.5 (XRP out/in)	B1/2	1/5	out	out	16.4/38.3	15.6/36.4	15.0/35.0
TCL.6 (XRP out/in)	B1/2	1/5	out	out	out	out	out

Table 2: 2018 ion run collimator settings for a normalised emittance of ϵ_N=3.5μm. L and R indicates the left and right jaw, respectively.

Collimator	**Beam**	**IR**	**Injection**	**FT (β^*=1 m)**	**Physics (β^*=50 cm)**
TCPs/TCSGs/TCLAs	B1	7	5.7/6.7/10	5.5(L)-5.0(R)/6.5/10	5.5(L)-5.0(R)/6.5/10
TCPs/TCSGs/TCLAs	B2	7	5.7/6.7/10	5/6.5/10	5/6.5/10
TCPs/TCSGs/TCLAs	B1/2	3	8/9.3/10	15/18/20	15/18/20
Horizontal TCTs	B1	1/2/5	13	15/15/15	11/9/9
Horizontal TCTs	B2	1/2/5	13	15/15/15	9/9/9
Vertical TCTs	B1/2	1/2/5	13	15/15/15	9/9/9
TCTs	B1/2	8	13	15.0	15
TCDQ	B1/2	6	8	7.4	7.4
TCSP	B1	6	7	7.4	7.4
TCSP	B2	6	7	7.4	7.4(L)-11.2(R)
TCL.4/5/6	B1/2	1/5	out	out	15/15/out

when the Roman Pot detectors (XRP) for forward physics are inserted, are also indicated.

An overview of the evolution of the collimator settings during Run 2 during the ion runs is also shown in Fig. 2b. The collimator settings for the ion runs are usually chosen to be the same as for the proton runs in all IRs except in the experimental areas to gain time in the set-up. In Table 2 the collimator settings for the 2018 ion run are summarised for the different points in the cycle.

In 2018 the collimation system has been operated with tighter-than-designed settings for both proton and ion beams achieving TCTs gaps as small as 7.8 σ. More details about the different Run 2 machine configurations and collimator settings can be found in [14].

COLLIMATION CLEANING PERFORMANCE

Validation procedure

For a given choice of the collimator settings the cleaning inefficiency and the hierarchy of the system are validated by means of betatron and off-momentum beam Loss Maps (LMs) before high-intensity beams are allowed. For the betatron LMs, losses are induced by blowing-up the beam in the transverse planes with the Transverse Damper (ADT) that can inject band-limited white noise into the beam. For the off-momentum LMs, off-momentum losses are induced by shifting the synchronous phase of the Radio Frequency (RF) system. The losses along the ring are recorded by the Beam Loss Monitoring (BLM) system. The validation for each set of collimator settings is completed by ABD tests [15], in order to validate the protection of the machine in such scenarios. These measurements are an essential part of the beam commissioning of the machine after long periods without beam or following relevant changes in the hardware or in the machine configuration. In the commissioning, the validation procedure consists of a complete set of betatron and off-momentum (both signs of frequency shift) LMs and ABD tests performed at each static point in the cycle. Along the run this validation needs to be repeated for each machine configuration involving a change of optics and/or collimator settings, after each Technical Stop (TS) happening along the year or every three months if the other two cases do not happen before. In these cases, the number of LMs to be performed is optimised, usually all betatron LMs have to be performed, but only one off-momentum frequency sign is repeated, which has to be alternated along the year. In addition, since 2016 continuous LMs are performed in dynamic beam processes such as the energy ramp and the β^*-function squeeze as part of the validation procedure. More detail on the optimised strategy and procedure can be found in [16,17]. The number of LMs required in the validation process has

increased along Run 2 due to the increased complexity of the LHC cycle, changes of configuration, special runs requested and the Machine Development (MD) tests requiring special collimator settings. In particular, in 2017 and 2018 the LMs required for the standard run validation increased due to the implementation of luminosity levelling methods. Figure 3 shows a summary of the LMs and fills, required and performed in 2018. Taking into account the LMs performed during MD time, in total 482 LMs were performed in 2018. Moreover continuous betatron LMs during the energy ramp were performed.

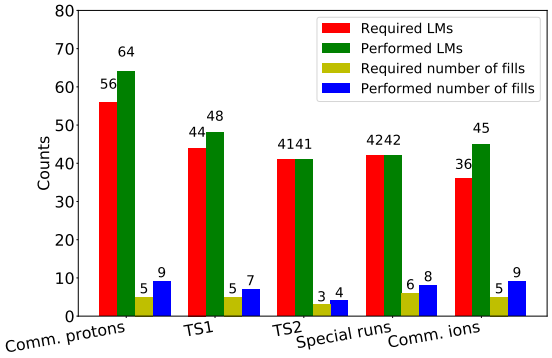

Figure 3: Summary of the number of LMs required (red), LMs performed (green), fills required (yellow) and fills performed (blue). The ABD tests are included in the counting of the number of fills required and performed.

At the start of Run 2, one fill per off-momentum LM was required. It was not possible to control the RF trim timing and a shift in frequency of ± 500 Hz was needed to have enough resolution, always causing the dump of the beam. In 2016-2017 a new FESA class [18] and GUI were developed to control the RF trim with a feedback loop based on the readings of the 100 Hz stream of BLM data. Off-momentum loss maps could be made in a more controlled way, with real time RF trims around ±150 Hz avoiding losing the full beam and hence re-using it for the next validation step. Still the FESA feedback was sometimes not able to prevent beam dumps. In 2018, a new GUI with a different implementation of the feedback was deployed which made the off-momentum LM-data taking easier, more automatic and in general the LM validation more efficient. The number of dumps occurring during the off-momentum LMs have been reduced in Run 2 and now the validation process is almost determined by the ABD tests required by the LHC Beam Dump System (LBDS) team.

Protons and ions cleaning

In Fig. 4, LMs for the full ring (left) and the zoom on IR7 (right) are shown for protons (top) and Pb ions (bottom) for Beam 1 in the horizontal plane and the 2018 physics optics. The losses are classified as cold (blue), warm (red), collimator (black) and XRP (green) losses. The cold losses refer to losses in the aperture of SC magnets while the warm losses refer to losses in normal conducting magnets and other equipment at room temperature. The BLM signals are normalised by the highest BLM signal, which is typically measured in IR7 where primary beam losses are intercepted. The highest cold spikes are found in two clusters downstream of the collimation system in the Dispersion Suppressors (DS) indicated in Fig. 4 as DS1, DS2 and DS3. For protons, good cleaning around the ring was observed, and the system was stable and reproducible along the year with only one collimator alignment campaign performed during the commissioning. In Fig. 5a the maximum normalised BLM signals measured in cold magnets for the two beams and planes are shown at different points in the cycle from all measurements performed in the commissioning, after TS1 and TS2. The points in the cycle considered in this plot are: injection, FT, End of the Squeeze (EoS), and physics with the XRP in and out. For the points in the cycle corresponding to the physics configuration, the first number corresponds to the β^*-function value and the second one to the crossing angle. During the validation processes in the beam commissioning, a hierarchy breakage in IR7 was observed for Beam 1 in the vertical plane at FT energy. Dedicated functions for all collimators are set up to connect the settings in each static point of the cycle to ensure a good performance of the collimation system also during dynamic phases such as the energy ramp and the optics squeeze. The problem was solved by implementing in all the beam processes the measured tilt angle of the TCSG.D4L7.B1 of -400 μrad and 320 μrad for the left and right jaw, respectively. This was crucial specially at FT energy. The point in Fig. 5a for Beam 1 in the vertical plane at the EoS performed in the commissioning corresponds to the LM performed without the secondary collimator tilt angle implemented. As already mentioned, continuous betatron loss maps are performed during the energy ramp and the squeeze beam processes as part of the collimation system validation since 2016. In Fig. 5b, the measured cleaning inefficiency in 2018 during the energy ramp for different energies is shown for both beams and both planes. An overview of the cleaning inefficiency in Run 2 at FT energy is shown for protons in Fig. 6a. The observed improvement of the cleaning inefficiency along the years is related to the tightening of the collimator settings in IR7 as can be seen in Fig. 2b.

Furthermore, the losses at the TCTs were analysed during the crossing-angle anti-levelling from 160 μm to 130 μm and the β^*-function levelling from 30 cm to 25 cm. Figure 7a and 7b shows an example of the measured normalised BLM signal at the TCTs during these beam processes for Beam 1 and Beam 2, respectively. No increase in losses at the TCTs is observed during the crossing angle changes as expected; on the contrary during the β^*-levelling, losses increase by up to a factor 2. The observed behavior was stable and reproducible along the year.

During the Pb ion run validation in the commissioning of 2018, some collimators had to be adjusted empirically because of too high losses observed. This was the case for the horizontal primary and tertiary collimators in IR1 for Beam 1 and for the TCSP in IR6 for Beam 2, as can be seen

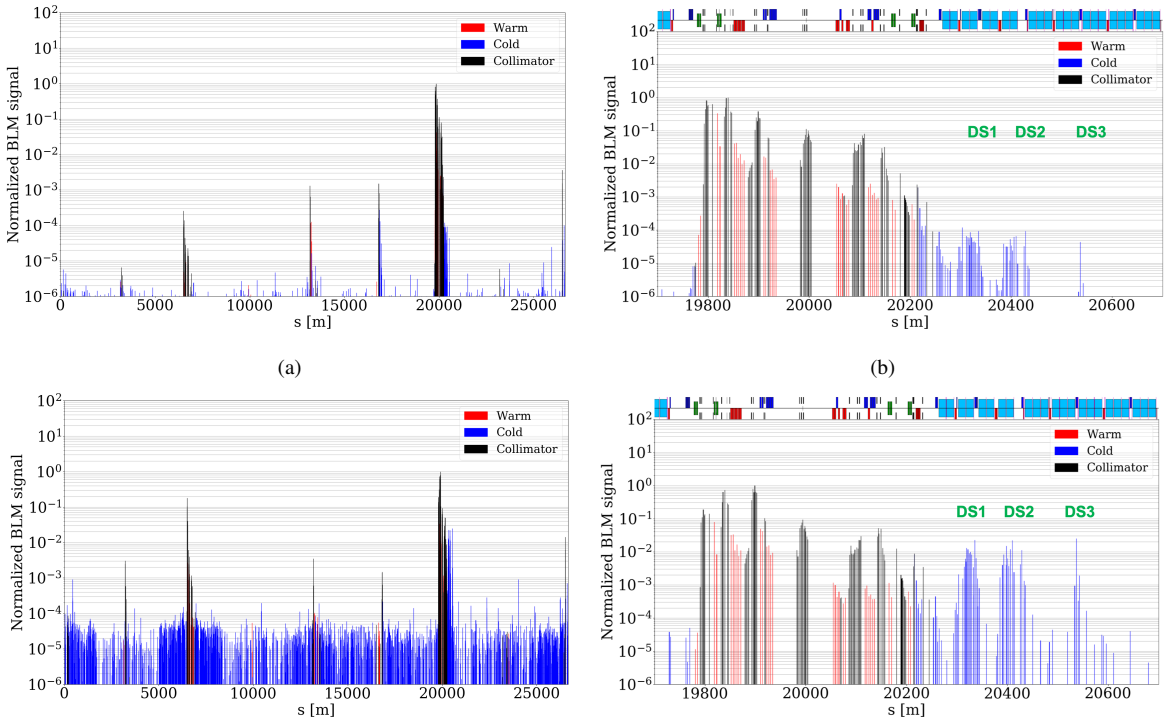

Figure 4: Proton (top) and Pb ion (bottom) full ring (left) and IR7 zoom (right) loss map performed with colliding beams in the horizontal plane for Beam 1.

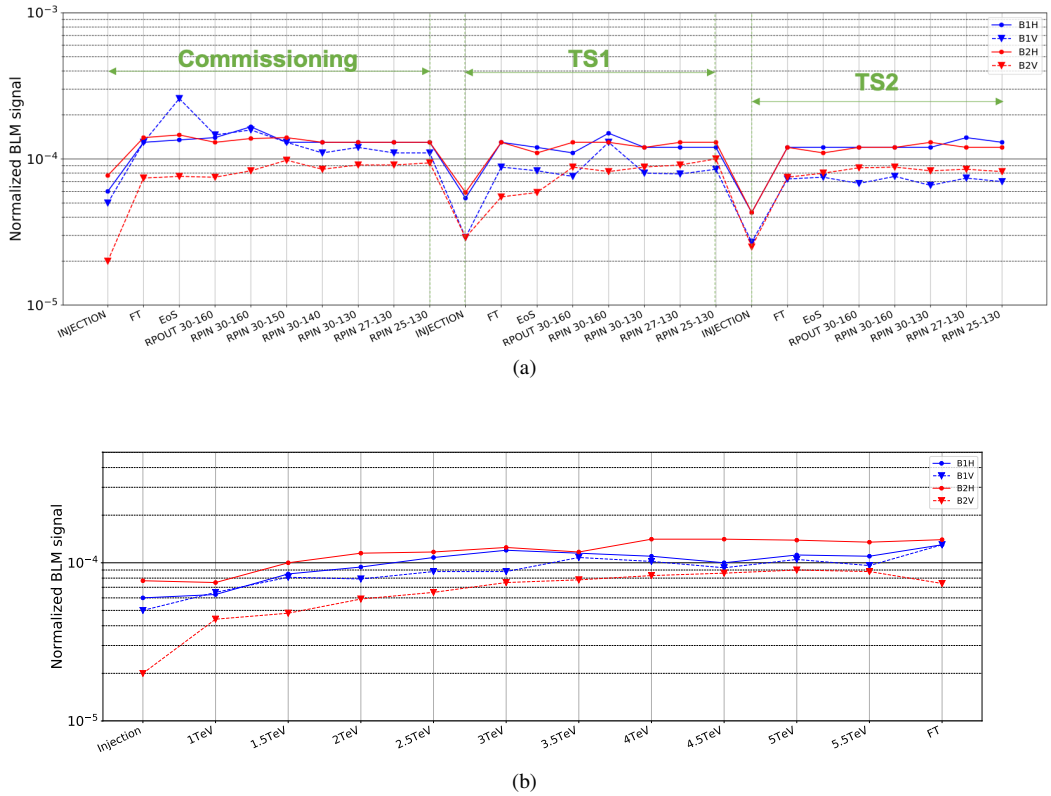

Figure 5: 2018 proton cleaning-inefficiency measurements at different static points in the cycle (a) and during the continuous ramp and squeeze beam process (b) for both beams and both planes.

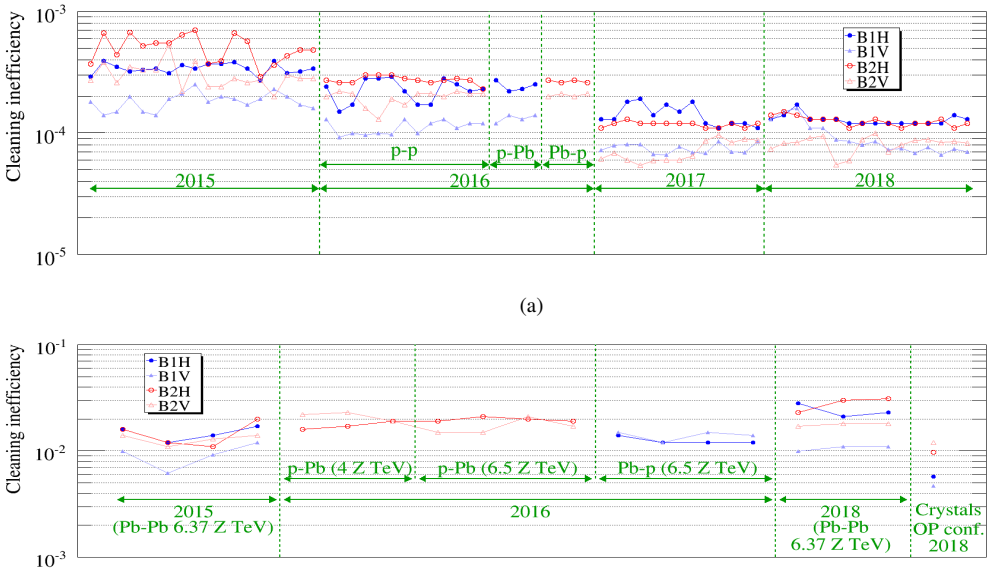

Figure 6: Run 2 proton (a) and ion (b) cleaning inefficiency at FT energy measured during the commissioning and TSs. The proton-proton physics runs were always operated at 6.5 TeV while the ion runs were operated with 6.37 Z TeV ion beams in 2015 and 2018 for lead-lead physics, and with 4 Z TeV and 6.5 Z TeV ion beams in 2016, for proton-lead physics.

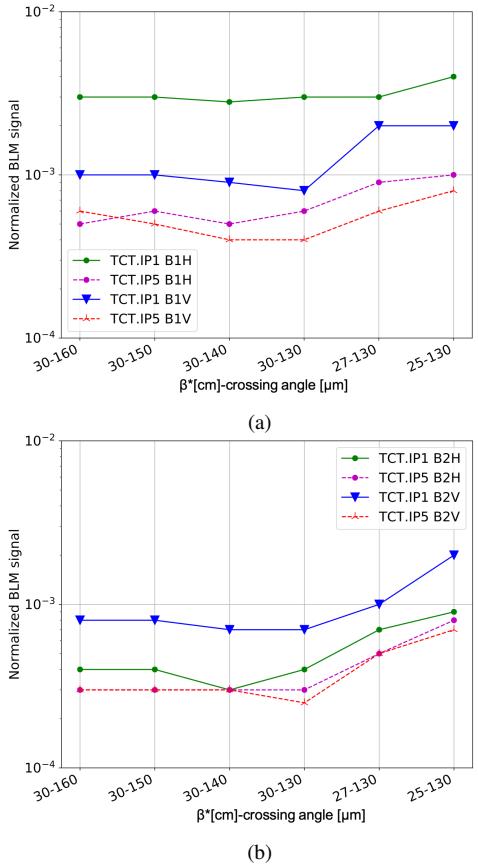

Figure 7: Normalised BLM signal at the TCTs measured during the 2018 beam commissioning for Beam 1 (a) and Beam 2 (b) during luminosity levelling beam processes.

in Table 2. For ions, a worsening of the cleaning inefficiency in the DS in IR7 was observed by more than two orders of magnitude with respect to protons, as can be seen in Fig. 4d. This is due to the difference in the interaction mechanisms in the collimators. Ions experience nuclear fragmentation, and hence a substantial flux of off-rigidity particles escape the collimation system. Moreover, an apparent breakage of the hierarchy is observed in IR7 where the highest observed BLM signal was of a TCSGs instead of the TCPs. This observation was further investigated experimentally to confirm that the signal at the TCSGs was coming from showers or secondary ion fragments and not from primary beam, meaning that the hierarchy was indeed correct in spite of the BLM pattern. Additional loss peaks were also observed in the arcs between IR7 and IR1 in local maximum values of the dispersion function as well as more losses in the off-momentum collimation cleaning insertion. The observed worsening in the cleaning inefficiency stresses the need of optimising and better understanding the collimation cleaning performance for ions in view of higher-intensity runs. Figure 8, summarises the maximum cleaning inefficiency in cold magnets for different points in the cycle. In addition, an overview of the cleaning inefficiency along Run 2 at FT energy is shown in Fig. 6b. A similar level of cleaning inefficiency is observed for the different ion runs, regardless change of energy and collimator settings. Thus, indicating that the present system is essentially working as a single stage collimation.

In 2018 a full program of tests were carried out with a new collimation scheme based on bent crystals. For the state of completeness, the measured cleaning inefficiency with this new scheme for ions is included in Fig. 6b. In general, the crystal-based collimation scheme was shown to improve

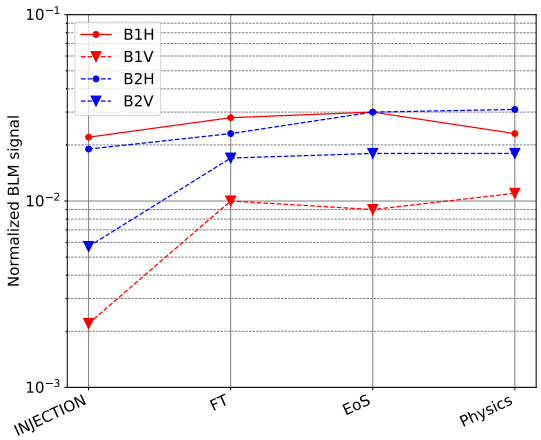

Figure 8: 2018 measured ion-cleaning inefficiency during the Pb ion beam commissioning for both beams in both planes all along the cycle.

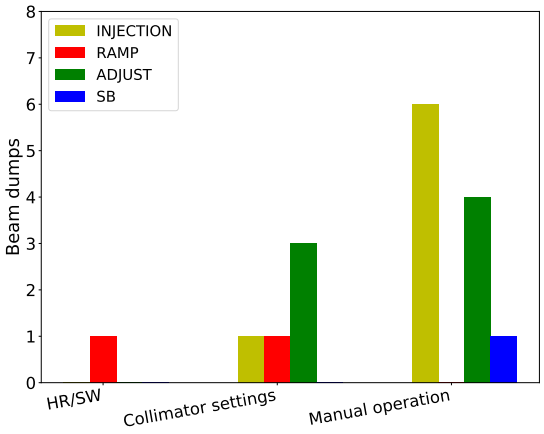

Figure 9: 2018 beam dumps related to the collimation system from the Post Mortem (PM) data base browser [20].

the cleaning efficiency. More information is given in the fifth section of this paper.

SYSTEM AVAILABILITY AND FAULTS

The availability of the collimation system was high throughout Run 2 with negligible machine downtime [19]. Figure 9 shows a summary of the collimation system related beam dumps in 2018. The causes of beam dumps in operation have been classified as hardware/software related, collimator settings errors, and manual collimator operation. The beam dumps at the different points of the cycle are shown with different colours. The human factor is the main collimator-related fault affecting primarily the commissioning and MD time, which reflects the complexity of the system. Only one dump was registered in 2018 from hardware/software issues [20] due to a wrong temperature sensor reading during the ramp in the ion run. More details on the occurrences in previous years are given in [7,21,22].

A detailed analysis of the collimator hardware-related faults was performed and presented in [23]. Figure 10 shows a summary focused on Run 2. The most frequent cause of failures during Run 2 was wrong readings of the temperature sensors. In order to improve this for future runs a new algorithm will be implemented during LS2 to recognise broken temperature sensors in real time. Moreover, at the beginning of Run 2, a high number of failures occurred on the Linear Variable Differential Transformer (LVDT) sensor and resolvers transducers due to the oxidation of National Instrument (NI) high-density cables. In order to solve this problem, in 2017 it was decided to launch a cleaning campaign of the cable connections in every year technical stop (YETS). This action reduced significantly these failures in 2017.

The operational experience and preventive maintenance have decreased the number of failures during the last years of operation despite the increased number of collimators

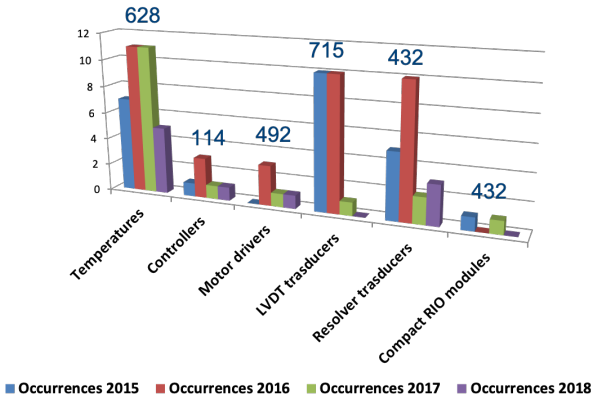

Figure 10: Run 2 analysis of the collimator-hardware-related faults [23]. The vertical axis in the chart shows the number of encountered faults per year and the number on the top of the bars corresponds to the current installed number of units.

installed. The Run 1 and Run 2 down time is summarised in Fig. 11. It was remarkably below 2 hours in 2017 and 2018. Concerning mechanical issues, only one occurred in 2018, related to a faulty attachment position of an LVDT sensor.

COLLIMATOR CONTROLS

Alignment

For the collimation system to work, the individual collimator jaws are centered around the beam. Each collimator has to be aligned at the extreme points of every beam process along the cycle that implies a collimator movement. In the 2018 proton commissioning a total of 199 collimator alignments were performed: 79 collimators at injection, 75 collimators at flat top, 16 collimators at the end of squeeze, and 29 collimators in physics.

The beam-based alignment (BBA) technique [24,25] is the main method used to align the collimators. The jaws

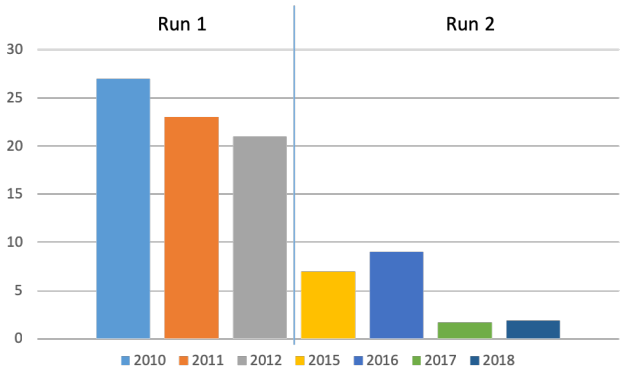

Figure 11: Run 1 and Run 2 down time caused by collimator-related faults [23].

of the collimator that should be aligned are moved towards the beam until they touch the halo of the circulating beam, inducing local losses at the collimator BLM; exceeds a predefined threshold such as the movement is stopped, and the expert identifies the loss spike as a signature of the collimator jaws touching the beam. This approach is time-consuming and prone to human errors, especially when a large number of collimators need to be aligned. As a result, the setup is not performed frequently and margins must be included when fixing the collimator settings to account for possible orbit drifts during the year. However this has not been a source of limitation so far, thanks to the good beam orbit stability.

During LS1, a total of 18 collimators were installed/replaced with collimators with BPMs embedded in each jaw corner. These collimators are aligned using the BPM signal of the 4 corners. Each collimator corner is moved until left and right jaw signals are equal for upstream and downstream corners, respectively [26]. Assets of the BPM-based procedure: faster than the BLM-based method since the time needed to align all collimators with BPMs is reduced from approximately one hour to a few minutes; moreover no beam particles are intercepted avoiding losses; in addition the alignment can be done at larger collimator gaps and the BPMs allow to reconstruct the beam-jaw angle.

Thanks to the use of the BPMs for the alignment of the TCTs, the time required in the commissioning was reduced as illustrated in Fig. 12. This was crucial in view of the increased number of configuration changes in the IRs in Run 2, requiring the alignment of the TCTs. In 2016, thanks to the availability of the 100 Hz BLM data for the BBA-alignment the time required was further reduced. Moreover, during Run 2, a lot of work has been performed in order to develop an automatic software for the BBA based method. In the 2018 commissioning, the first version of a fully-automatic software was tested and all collimators were successfully aligned in all cycles of the machine in 5 hours. The automation is based on machine learning to detect automatically spikes corresponding to the collimator jaws touching the beam. In addition, the software also includes an automatic threshold selection algorithm based on real-time 100 Hz BLM data. A summary of the 2018 results can be found in [27, 28].

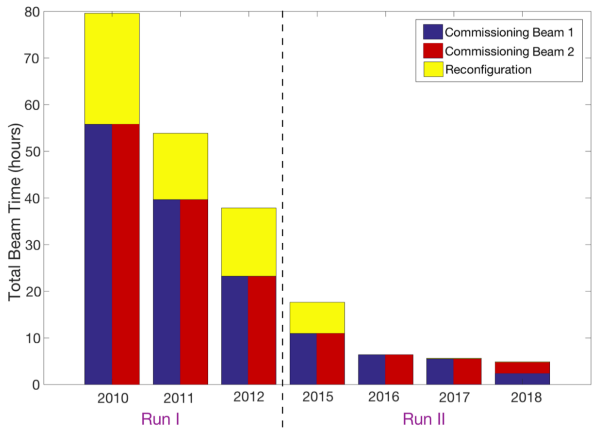

Figure 12: (a) Time required to align the full collimation system during Run 1 and Run 2 alignment campaigns [27].

The first version of this software did not account for cross-talk between the beams, therefore the two beams could not be aligned in parallel during the 2018 proton run commissioning. After the commissioning, an initial cross-talk analysis model was developed and integrated into the fully-automatic software. The new parallel fully-automatic software was tested during the MD 3343 [29]. All collimators on both beams were successfully aligned at injection in 50 minutes. Figure 13 shows the comparison of the time needed to align all collimators at injection with the semi-automatic and the fully-automatic software with and without parallelisation. The cross-talk model used will be further upgraded based on more in-depth cross-talk analysis studies [30].

During Run 1 and Run 2 the collimators were aligned without taking into account the divergence of the beam, however, the tank misalignment and/or the large beam envelope angles can introduce a tilt that could limit the collimation system performance. A series of MDs were carried out in 2016 [31, 32] and 2017 [33] to asses the stability of the alignment and the limit in the operational margins. These MDs show a hierarchy breakage on Beam 1 in the vertical plane when the TCP-TCSG retraction was set to 1 σ which corresponds to the foreseen nominal LHC retraction. In these MDs it was also observed that the hierarchy could be restored by implementing the tilt angle of the jaws of TCSG.D4L7.B1. Furthermore, in 2018 even with 1.5 σ retraction a breakage of the hierarchy was observed and the tilt angle of TCSG.D4L7.B1 had to be implemented in normal operation for a good preservation of the collimation system hierarchy. The angular alignment is a key element for envisaged operation with tighter margins between the primary and the secondary collimators. Three semi-automatic angular alignment methods have been fully automated in 2018 and they have been successfully tested during MD 3344. The detailed description of the methods and the main results can be found in [34, 35].

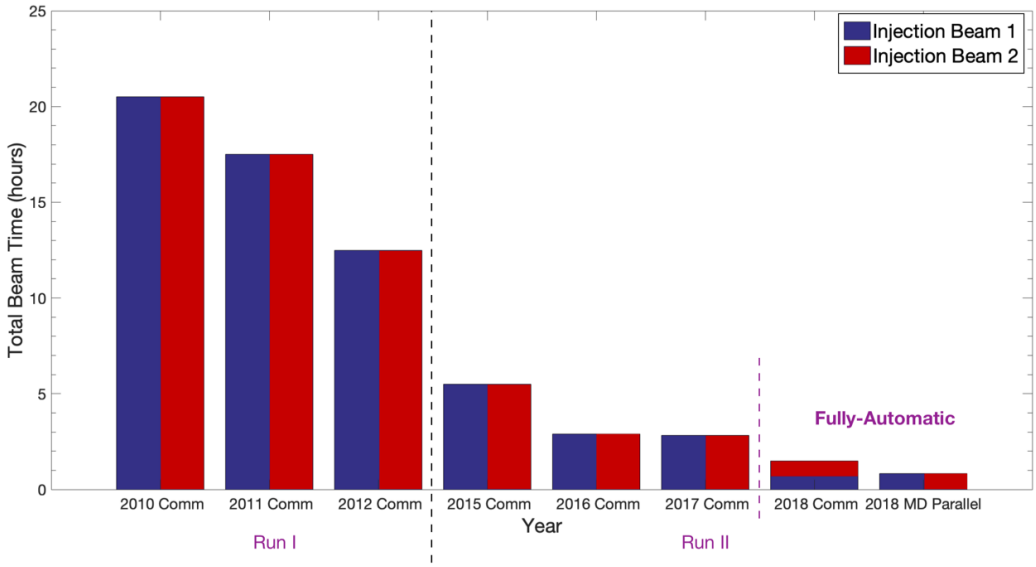

Figure 13: Comparison of the time needed to align all collimators at injection with the semi-automatic and the fully-automatic software with and without parallelization [27].

Collimator BPM performance

In 2018, the LHC layout contained a total of 22 collimators with embedded BPMs (all TCTs, the TCSPs in IR6, the TCLs with wires in IR1 and IR5 and the horizontal TCP for Beam 1 and the TCSPM prototype in IR7), which are very important for collimator alignment and monitoring. Their importance for alignment has been already stressed previously. The orbit monitoring at the collimators allows checking the relative beam-jaw position, the fill-to-fill reproducibility and to add interlocks to the machine. Orbit interlocks at the collimators were implemented for the first time in 2017 in the Software Interlocks System (SIS). In addition, redundant BPM readings were added in 2018 in order to make the interlock system more robust. For the 2018 operation the interlocks were set to 1 σ in IR1/5, 2.5 σ in IR8 and 1.5 σ in IR6. During the 2017 and 2018 operation runs the orbit monitoring and interlocking were very important to protect the machine during the anti-levelling crossing angle beam process and to allow the tightening of the TCSP-TCT margins.

Good stability and reproducibility of the BPM readouts have been observed all along the 2018 operation as well as a good fill-to-fill reproducibility. Furthermore, no spurious interlocks had been triggered provoking premature beam dumps [36]. This is a very important achievement since the system was not designed for this purpose. In Fig. 14 an example of the BPM signal during the energy ramp beam process for all 2018 proton fills is shown in comparison with the MADX model in black. As can be seen, the behaviour of the beam is well reproduced by the TCT function. Fig. 15 shows an example of the maximum orbit excursion in all IPs for all 2018 proton run fills is shown for Beam 1 (top) and for Beam 2 (bottom) at different points in the cycle (ramp, squeeze, adjust and stable beams). In IR5 a degradation of

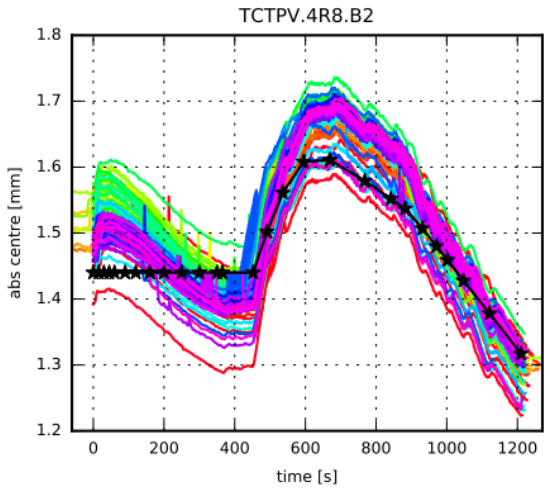

Figure 14: Example of 2018 BPM signal during the energy ramp beam process for all the proton run fills in different colours in comparison with the MADX model in black.

the centre in the horizontal TCT was observed increasing during the year and along the LHC cycle. This behaviour should be better understood in the future but it was still well inside the interlock limit.

Stability of collimator jaw positions

The LVDT sensors are installed in the collimators to measure the jaw positions and gaps (6 units per collimator). The readings of the LVDTs are regularly checked for all movable collimators as a part of the Machine Protection (MP) checklist during the intensity ramp up and the physics production. Figure 16 shows the number of collimators exceeding a 30 μm threshold on the LVDT reading with respect to the motor position for all the fills in 2018. In 2018 this monitoring

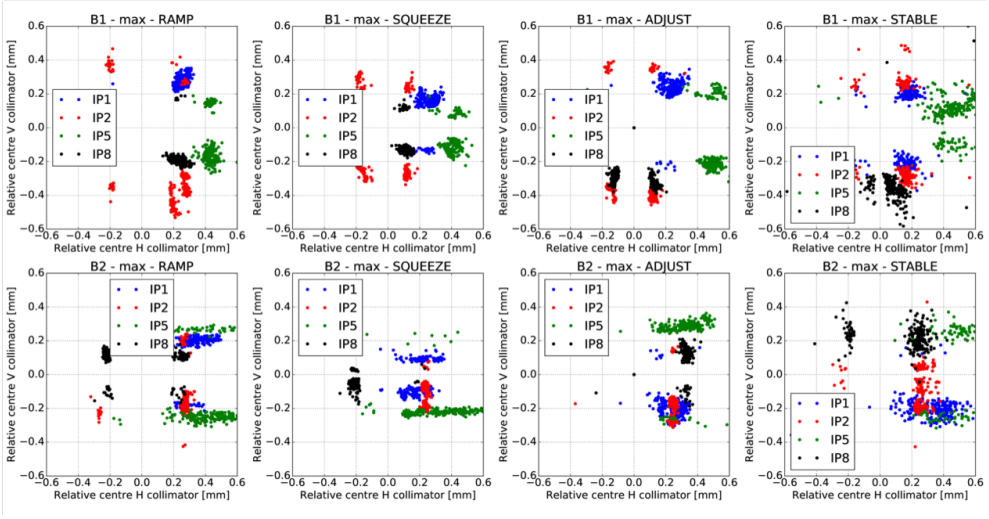

Figure 15: Maximum orbit excursion in all the IPs for all proton run fills for different points in the cycle (ramp, squeeze, adjust and stable beams) for Beam 1 (top) and for Beam 2 (bottom)

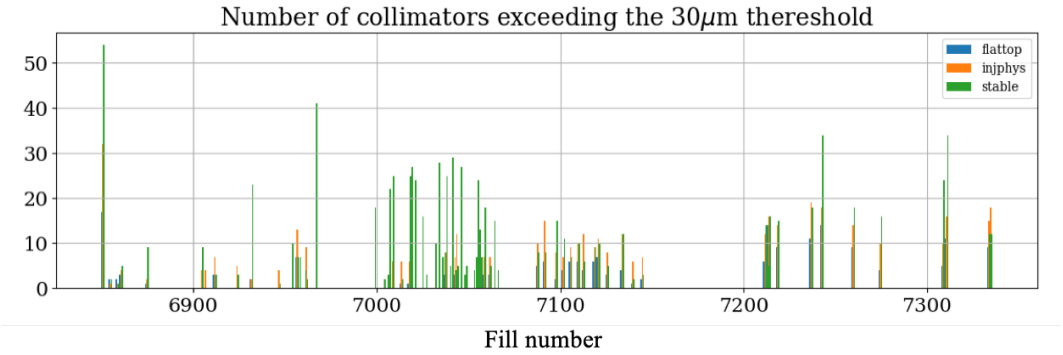

Figure 16: Number of collimators exceeding a 30 μm threshold of the LVDT reading with respect to the motor position for all the 2018 fills. Notice that the MD periods have not being included in this analysis.

served to detect a few anomalies during operation spotting the use of wrong settings after the MD period (see the two highest spikes in Fig. 16). In general, for both proton and ion runs the maximum drifts observed are about 200 μm, and in the vast majority of the cases well below 100 μm. An excellent reproducibility was attained from the mechanics and electronics point of view.

EXPERIENCE WITH NEW COLLIMATOR HARDWARE

New collimator hardware was installed in LS1 and during each yearly stop for tests and design validation with beam in the framework of the High Luminosity Large Hadron Collider (HL-LHC) project [37] and to explore new collimation system schemes. A complete crystal-based collimation system was installed (one crystal per beam and per plane), as well as a low-impedance TCSPM prototype, four collimators with embedded wires and a TCP with embedded BPMs on Beam 1. The new hardware had no impact in the availability and performance during standard operation and tests were successfully performed. In the following paragraphs the most relevant achievements with these devices are summarised.

Crystal-based collimation system

In this new collimation scheme a bent crystal is used as a primary collimator. The beam halo particles are channeled between the crystal planes and deflected into a secondary collimator. In LS1, two crystals were installed on Beam 1 and the system was finally completed in 2017 with two more crystals on Beam 2. First tests were performed with proton and Pb ion beams in 2015-2017 [38, 39]. In 2018 several MDs were dedicated to study operational aspects of the full system with proton (MD 3327 and MD 4168) [40,41] and ion beams (MD 4167) [42]. All crystals have been characterised and a complete loss map campaign was performed with different settings to assess the efficiency of the system as a function of the collimator settings. In addition, the crystals were kept in channeling during dynamic operational phases such as the energy ramp and the squeeze. Moreover, some tests were performed as part of the intensity ramp up during the Pb ion run commissioning and the crystals were inserted with 640 bunches and operationally deployed for several

hours at the end of the fill and more details on the tests performed are given in [43, 44].

With the crystal-based collimation system, in general an improvement of the cleaning inefficiency in the IR7 DS and along the ring is observed with respect to the standard collimation system cleaning. The improvement is more significant for Pb ions due to the worsening observed with the standard collimation system with respect to protons. Figure 17a and 17b shows the measured loss maps with the crystal-based collimation and with the standard collimation system, respectively, for Beam 1 in the horizontal plane. Detailed analysis of all the data collected during the year is ongoing.

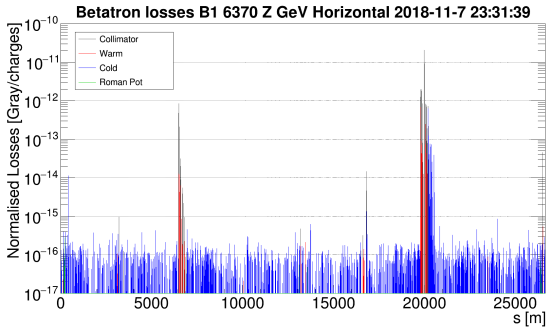

(a)

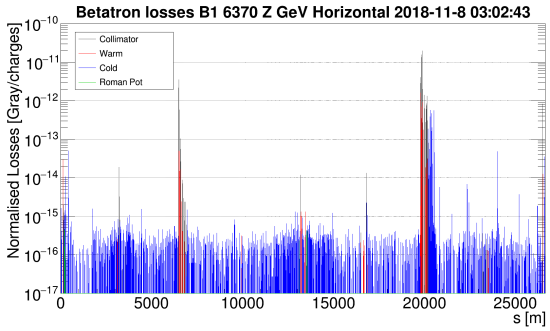

(b)

Figure 17: Crystal-based collimation system (a) and standard collimation system (b) LM for Beam 1 in the horizontal plane.

Furthermore, the performance of the system was investigated by means of simulations and experimental tests to asses the special high-β^* physics run. The crystal-based collimation system was used in operation successfully for the first time in physics [43, 44]. More details are given in the next section.

TCSPM collimator prototype

In 2017, a TCSPM collimator prototype was installed in the LHC on Beam 2 in a slot adjacent to the secondary collimator TCSG.D4R7.B2 [45]. The jaws of the TCSPM collimator prototype are made of MoGr and the surface of the jaw is coated with three different materials (Mo, MoGr and TiN) in separated stripes as can be seen in Fig. 18.

An extensive campaign of tune-shift measurements with all TCSPM coating materials was performed during 2017

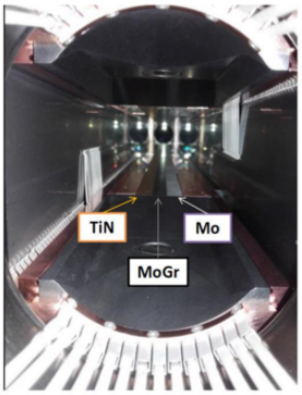

Figure 18: TCSPM prototype with the different coatings materials indicated.

and 2018 to benchmark impedance models against measurements. A reduction of the impedance was observed as expected from the theoretical models for the MoGr coating [33], but some discrepancies were observed between measurements and the theoretical models. Further investigations were performed and the source of the discrepancies was found in the micro-structures of the coating. The experience gained has been incorporated in to the design specification of the TCSPM coating layer. These new secondary collimators will be installed in LS2.

The TCSPM prototype has been used as an operational collimator at nominal settings in 2018. The detailed analysis of the performance of the TCSPM-prototype was reported in [46]. For all the 2018 proton fills, the sum of the TCSPM adjacent BLM signal divided by the time duration of the particular point of the cycle (adjust, energy ramp, squeeze and stable beams) is shown in Fig. 19a in comparison to the BLM signal of the closest secondary collimator. No significant differences were observed between the signals at the TCSG and the TCSPM. Furthermore, the analysis of the temperature of the two jaws for the different points in the cycle is also shown in Fig. 19b for the proton run. The temperature fluctuations observed along the year are within one degree for protons and below half a degree for ions. The jaw position reading from the LVDTs all along the ramp were also monitored and were found to be very stable over all the fills. The TCSPM prototype jaw movement was very reproducible and no abnormal behaviors were observed. Altogether, despite of some initial concerns about the vacuum point of view the prototype worked very well in all aspects relevant to operation.

Collimators with embedded wires

One tertiary collimator (TCTPH.4R5.B2) and a collimator for physics debris (TCL.4L5.B2) were replaced on Beam 2 in IR5 by tungsten collimators with in-jaw wires in 2016 [47]. The goal was to demonstrate that it is possible to compensate or alleviate the long-range beam-beam effects by powering the DC wires in the framework of the HL-LHC project. In addition in 2017, two other collimators were replaced in

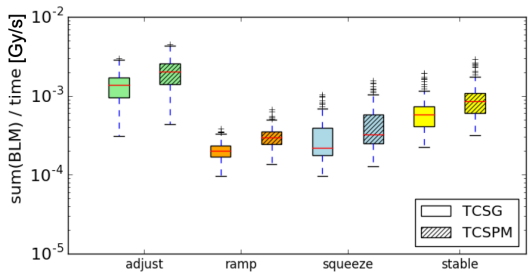

(a)

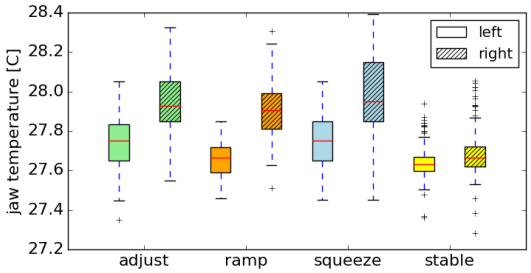

(b)

Figure 19: (a) TCSPM and TCSG adjacent BLM signal sum divided by the time duration of the particular point of the cycle (adjust, energy ramp, squeeze and stable beams) for all the 2018 proton fills. (b) TCSPM temperature monitoring at the different points of the cycle for all the proton run fills. In this plot the boxes extend from the lower to upper quartile values of the data with a red line at the median. The whiskers extend from the box to show the range of the data between the maximum and minimum values.

Beam 2 in IR1 (TCTPV.4R1.B2 and TCLVW.AL5.B2). In 2017 and 2018 an extensive experimental campaign carried out and the main results published in [48]. During the MDs the collimators could be used reliably at high wire current. The performance of these collimators was smooth and reliable all along the run and no impact was observed during normal operation. These collimators will remain in the LHC for Run 3 but they will be moved to different locations [49].

TCP.C6L7.B1 with embedded BPMs

The horizontal TCP for Beam 1 (TCP.C6L7.B1) was replaced in 2017 by a prototype equipped with BPMs [50] in order to consolidate this collimator design for the future LHC TCPs. These collimators are exposed to a high radiation dose and it was important to test the performance of the embedded BPMs with beam. A very good performance of the prototype and the embedded BPMs was observed all along the 2017 and 2018 operation.

COLLIMATION PERFORMANCE DURING SPECIAL RUNS

The LHC collimation system is essential also for special runs such as the van der Meer scans, for precise luminosity calibrations, and the high-β^* runs, for forward physics. In particular, in 2018 the research and work performed on the development of an optimum collimation scheme made it possible to accomplish the goals of the high-β^* run physics program experiments at injection. In this section we will focus on the main achievements during the high-β^* run physics.

Collimation performance during high-β^* runs

The LHC forward physics program of CMS-TOTEM and ATLAS-ALFA requires special high-β^* optics [51]. In this configuration, the beam is de-squeezed (the β^*-function at the collision point of the high luminosity experiments ATLAS and CMS is increased) in order to minimise the divergence at the IP to measure the proton-proton elastic-scattering at small angles. In these low beam intensity runs, the XRP detectors located at about 200 m from the IPs are placed as close as possible to the beam. Special collimator settings are needed in order to minimise the aperture budget tighten by the collimation system while granting a satisfactory performance. The main role of the collimation system during the high-β^* runs is to reduce experimental background and not to protect the machine because the intensity is very low.

In Run 1, a large amount of background was present at the XRPs, which made the data analysis more difficult. In Run 2, a different collimator configuration was proposed in order to reduce the background at the XRPs. In the 2016 high-β^* run at 6.5 TeV, a single-stage system was used with a tungsten collimator as a primary stage [52]. This scheme was not sufficient for the 2018 high-β^* run at injection energy, where far too high backgrounds were observed at the ALFA experiment in initial tests. Therefore, a new two-stage cleaning system was developed, fitting both the primary and secondary collimation stages (both made of tungsten collimators), as well as the XRPs, within 0.5 σ. Figure 20 shows the 2018 collimation system settings deployed in units of beam size, σ.

In addition, the novel collimation crystal-based system was investigated by means of simulations and experimental tests. In this configuration, the crystals replace the primary collimators and TCTs are used for the secondary collimation stage. Promising results were obtained, and in the last 2018 special physics run the crystal-collimation scheme was used in operation in combination with the standard collimation system. The beam intensity during the last 2018 high-β^* run is shown in Fig. 21 where the fills operated with the standard and crystal-based collimation system are indicated. The two systems could be alternated in a very efficient way.

Very good results were obtained with both schemes providing a reduction of the background in the ALFA experiment by a factor 1000. The standard system worked well for both experiments but an increase of the background was observed with time due to the repopulation of the beam halo. This problem was solved by performing beam halo scrapings. With the crystal-based system there was no need to perform the scrapings. The crystal-based system provided excellent results for TOTEM for both background rate and

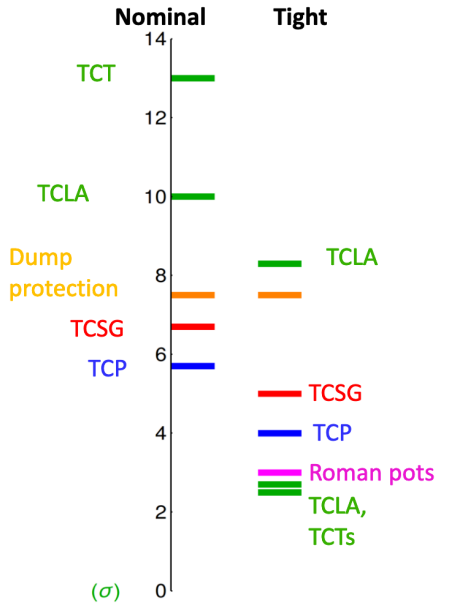

Figure 20: High-β^* run collimator settings in comparison to the 2018 nominal settings for high-luminosity physics. Note that for the high-β^* run the gaps in mm are still larger than for the nominal high luminosity physics ones.

distribution. For ALFA the background rate was improved but a problematic distribution was observed. The latter, was further investigated and the origin of the problematic spatial background distribution identified. The data could be used by applying some analysis and the settings can be optimised in the future to improve also the background distribution of the ALFA experiment [53].

RUN 3 COLLIMATION LAYOUT AND OPERATIONAL IMPLICATIONS

In the framework of the HL-LHC consolidation project, the LHC collimation system will undergo relevant upgrades [54] during LS2 to deal with the brighter beams foreseen by the upgrade of the injectors (LIU) [55].

The main upgrades aim to reduce the impedance induced by the collimation system and to improve the beam halo cleaning in IR7. In order to reduce the impedance, two new primary collimators with jaws made of MoGr and four secondary collimators with Mo-coated MoGr jaws will be installed for each beam in IR7. All new collimators have been designed with embedded BPMs. In order to improve the cleaning one dipole magnet per side of IR7 will be replaced by two 11 T dipoles with a TCLD collimator in between. In addition, a TCLD collimator per beam, without the 11 T dipoles, will be installed in IR2 for the heavy-ion runs. These collimators aim to absorb the Bound Free Pair Production (BFPP) secondary beam produced in the lead ion collisions [56–59]. The BFPP beam is lost in the DS after the IP and such losses increase the quench risk in the DS SC magnets and limits the achievable Pb luminosity. For ATLAS and CMS a method based on orbit bumps was implemented for the first time in 2015 to move the losses from the SC magnets to the empty connection cryostat. In 2018, this method was also used and provided a very good performance with a maximum peak luminosity reached in ATLAS and CMS of $6{\times}10^{27}$ cm^{-2} s^{-1} (the HL-LHC design luminosity is $7{\times}10^{27}$ cm^{-2} s^{-1}). In IR2, this solution does not work because of the different quadrupole polarities in the different IRs and because of that the TCLDs will be installed.

In addition, in IR7 the MQWA.E5[L,R]7 magnets will be replaced by shielding and a passive absorber because of the expected risk of failing since they are highly exposed to radiation. The powering of the Q5 modules will be re-configured to restore a proper optics. The change is necessary to limit the dose to the first module and re-establish a sufficient pool of spares.

From the operational point of view, after LS2, all the new collimators, such as the TCPs and TCSPMs with embedded BPMs and the TCLDs based in a new design, will have to be commissioned without and with beam. The collimator embedded BPM system will have to be validated for good polarities and position measurements including the new systems. Furthermore, the new hardware logging variables will have to be implemented in LSA and in the data base and the performance of the collimator controls validated as well.

CONCLUSIONS

For both protons and Pb ions the performance of the collimation system was very good all along Run 2 accommodating higher stored energies and many different machine configurations as can be seen in Fig. 6. For protons, the cleaning inefficiency was improved thanks to the tighter collimator settings implemented progressively. For Pb ions the cleaning performance of the collimation system was similar all along Run 2 but the stored beam energy was higher in 2018 and 7 out of 48 fills were dumped by high losses in the betatron-cleaning insertion caused by orbit oscillations at frequencies of about 10 Hz whose origin is under investigation. This underlines the need for a solution for future runs at higher intensity. In the short heavy-ion runs, the availability is crucial and every fill contributes significantly to the total integrated luminosity. For both, proton and ion runs, the stability, reproducibility and availability of the collimation system was very good. In 2017 and 2018 the downtime caused by collimator-related hardware was below 2 hours. This was very important for operation and very remarkable for a system in a high radioactive environment.

Relevant improvements have been made for speeding up the commissioning activities especially concerning the alignment of the collimators. A fully-automatic parallel collimator alignment software has been developed and validated as well as a fully-automatic angular alignment software. This could be crucial for tightening the hierarchy margins in future operations.

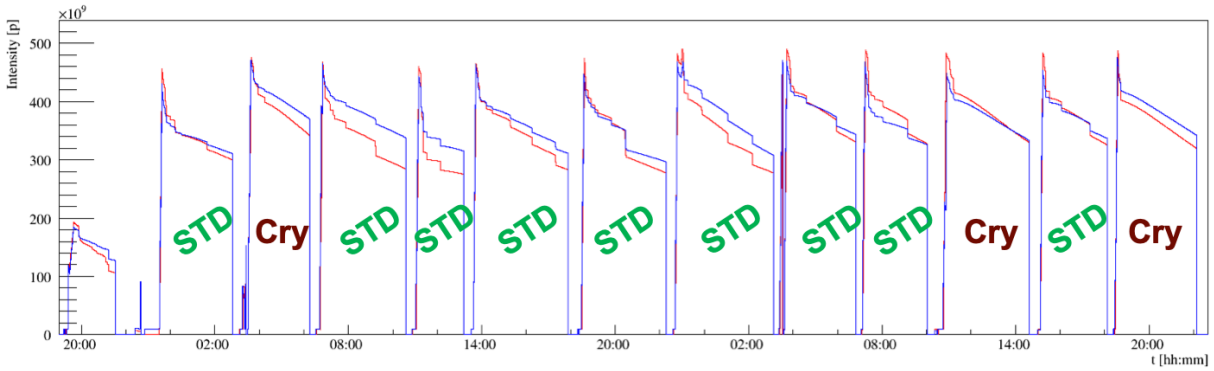

Figure 21: Beam intensity during the 2018 high-β^* run where the fills operated with the standard (STD) and crystal-based (CRY) collimation system are indicated.

New collimation hardware has been installed in Run 2 to consolidate the design of collimator prototypes in view of the HL-LHC project as well as to perform R&D towards new collimation schemes. The crystal-based collimation scheme provided in general an improvement of the cleaning inefficiency and was used operationally for the first time in the last 2018 high-β^* physics run.

Part of the HL-LHC hardware upgrades will be installed during LS2 and will contribute to dealing with brighter beams in Run 3.

ACKNOWLEDGMENT

The authors would like to thank colleagues in the BE-OP, BE-ABP, BE-BI, EN-STI and EN-SMM groups for all the help and support all along Run 2.

REFERENCES

[1] O. Bruning *et al.* (eds), "LHC design report", Vol. I, CERN, Geneva, Switzerland, Rep. CERN-2004-003-V-1, 2004.

[2] R. W. Assmann, "Collimators and beam absorbers for cleaning and machine protection", in Proceedings of the LHC Project Workshop – Chamonix XIV, Chamonix, France, 2005, p. 261.

[3] G. Robert-Demolaize, "Design and performance optimization of the LHC collimation system (Ph.D. thesis)", Universite Joseph Fourier, Grenoble, 2006.

[4] R. W. Assmann *et al.*, "The final collimation system for the LHC", Proceedings of the European Particle Accelerator Conference 2006, Edinburgh, Scotland, 2006, p. 986.

[5] C. Bracco, "Commissioning scenarios and tests for the LHC collimation system (Ph.D. thesis)", EPFL Lausanne, 2008.

[6] R. Bruce *et al.*, "Simulations and measurements of beam loss patterns at the CERN large hadron collider", Phys. Rev. ST Accel. Beams, 17 (2014), p. 081004, 10.1103/PhysRevSTAB.17.081004. http://link.aps.org/doi/10.1103/PhysRevSTAB.17.081004.

[7] G. Valentino, "Performance of the LHC collimation system during 2015", in proceedings of the 7th Evian Workshop, Evian, France, 15th-17th December 2015.

[8] B. Salvachua-Ferrando *et al.*, "Overview of Proton Runs During Run 2", in these proceedings, January 2019.

[9] D. Mirarchi *et al.*, "Special Losses", in these proceedings, January 2019.

[10] P. Hermes *et al.*,"Measured and simulated heavy-ion beam loss patterns at the CERN Large Hadron Collider", Nucl. Instrum. Methods Phys. Res., A, 819, 73-83. 11 p (2016). http://cds.cern.ch/record/2239699.

[11] R. Bruce *et al.*, "Reaching record low-β^* at the CERN Large Hadron Collider using a novel scheme of collimator settings and optics", Nucl. Instrum. Methods Phys. Res. A, January 2017, pag. 19 - 30, vol. 848, http://dx.doi.org/10.1016/j.nima.2016.12.039.

[12] R. Bruce *et al.*, "Detailed IR Aperture Measurements", CERN-ACC-NOTE-2016-0075, CERN, Geneva, Switzerland (2016).

[13] S. Fartoukh, "Achromatic telescopic squeezing scheme and application to the LHC and its luminosity upgrade", Phys. Rev. ST Accel. Beams 16, 111002 – Published 19 November 2013.

[14] R. Bruce *et al.*,"LHC Run II machine configurations", in these proceedings, January 2019.

[15] W. Bartmann, C. Bracco, M. Fraser, "Asynchronous dump validation test", LHC Operational procedure, EDMS-1698830,2016-06-08.

[16] B. Salvachua *et al.*,"Collimation qualification needs after TS", presented in the 115th meeting of the LHC Machine Protection Working Group, 28.08.2015.

[17] D. Mirarchi *et al.*, "Collimation: Experience and performance", in proceedings of the 7th Evian Workshop, Evian, France, 13th-15th December 2016.

[18] M. J. Wyszynski, "FESA class for off-momentum lossmaps and decomposition of beam losses at the LHC", CERN-ACC-NOTE-2017-0043, CERN, Geneva, Switzerland, 2016.

[19] B. Todd *et al.*, "LHC & Injectors Availability Run 2", in these proceedings, January 2019.

[20] https://apex-sso.cern.ch/pls/htmldb$_$dbabco/f?p=117:1:102165635729068.

[21] A. Mereghetti *et al.*, "Performance of the collimation system during 2016 -Hardware perspective", in proceedings of the

7th Evian Workshop, Evian, France, 13th-15th December 2016.

[22] A. Mereghetti *et al.*,"Beam losses, lifetime and collimator hierarchy", in proceedings of the 8th Evian Workshop, Evian, France, 12th-14th December 2017.

[23] M. Di Castro, "Overview of LHC Collimator Failures for Sensors, Motors and Main Controls Components", LHC Collimation Working Group, 4th February 2019, CERN, Geneva, Switzerland.
https://indico.cern.ch/event/792567/.

[24] G. Valentino *et al.*, "LHC Collimator Alignement Tool", Proceedings of ICALEPCS2013, San Francisco, CA, USA, TUPPC120.

[25] G. Valentino *et al.*, "Semiautomatic beam-based LHC collimator alignment", Phys. Rev. ST Accel. Beams, 2012, 051002,15,4.
http://prst-ab.aps.org/abstract/PRSTAB/v15/i5/e051002.

[26] G. Valentino *et al.*, "Successive approximation algorithm for BPM-based LHC alignment", PRST-AB 2013, Phys. Rev. ST Accel. Beams 17, 021005.

[27] G. Azzopardi *et al.*, "Operational Results of LHC Collimator Alignment using Machine Learning", Proceedings in the International Particle Accelerator Conference IPAC19, 19th-24th May, Melbourne, Australia.

[28] G. Azzopardi *et al.*, "Operational Results on the Fully-Automatic LHC Collimator Alignment", Physical Review Accelerators and Beams, 2019.

[29] G. Azzopardi, B. Salvachua, G. Valentino, "MD3343 – Fully-Automatic Parallel Collimation Alignment using Machine Learning", CERN-ACC-NOTE-2018-0071.

[30] G. Azzopardi *et al.* "MD1653-Part 1: Characterisation of BLM Response at Collimators", No. CERN-ACC-NOTE-2018-0070. 2018.

[31] A. Mereghetti *et al.*, "MD1447-β^*-reach: IR7 Collimation Hierarchy Limit and Impedance", report in preparation.

[32] A. Mereguetti *et al.*,"β^*-reach-IR7 Collimator Hierarchy Limit and Impedance",CERN-ACC-NOTE-2016-0007, CERN, Geneva, Swtzerland, 2016.

[33] A. Mereghetti *et al.*,"MD2191-β^*-reach: IR7 Collimation Hierarchy Limit and Impedance", report in preparation.

[34] G. Azzopardi *et al.*, "Automatic angular alignment of LHC collimators", in Proceedings of ICALEPCS2017, Barcelona, Spain, pp. 928–933, 2017.

[35] G. Azzopardi, B. Salvachua, G. Valentino, "MD3344 – Fully-Automatic Angular Alignment of LHC Collimators using Machine Learning", CERN-ACC-Note-2018-0083.

[36] A. Mereghetti *et al.*,"Analysis of collimator BPM",LHC Collimation Working Group 238, 28th of January 2019, https://indico.cern.ch/event/791354/, CERN, Geneva, Switzerland.

[37] G. Apollinari, I. Bejar Alonso, O. Bruning, M. Lamont, L. Rossi (eds.),"High Luminosity Large Hadron Collider (HL-LHC) Technical Design report V.01", Geneva, Switzerland, EDMS n. 1723851 v.0.71.

[38] R. Rossi *et al.*, "Crystal Collimation Cleaning Measurements with Proton Beams in LHC", MD Note, CERN-ACC-Note-2018-0024-MD, 2018.

[39] R. Rossi *et al.*, "Crystal Collimation with Lead Ion Beams at Injection Energy in the LHC", MD Note, CERN-ACC-NOTE-2018-0004, 2018.

[40] M. D'Andrea *et al.*,"MD3327 – Crystal collimation tests with proton beams", report in preparation.

[41] M. D'Andrea *et al.*,"MD4167 – Operational aspects of crystal collimation with proton beams", report in preparation.

[42] M. D'Andrea *et al.*, "MD3327 – MD4168 – Crystal collimation tests with Pb ion beams", report in preparation.

[43] D. Mirarchi, *et al.*,"Crystal collimation for lead ion beams", International Review of HL-LHC Collimation System, 11th-12th February, 2019, CERN, Geneva, Switzerland.

[44] M. D' Andrea *et al.*, "Preliminary results from crystal collimation studies in 2018", 70th HL-LHC TCC.
https://indico.cern.ch/event/804616/.

[45] R. Bruce and S. Redaelli, "Installation of a low–impedance secondary collimator (TCSPM) in IR7", EDMS doc. 1705738, LHC–TC–EC–0006, CERN,Geneva, Switzerland (2016).

[46] M. Patecki, *et al.*, "Operational experience with the TCSPM prototype", LHC Collimation Working Group, 4th February 2019, CERN, Geneva, Switzerland.
https://indico.cern.ch/event/792567/.

[47] A. Rossi *et al.*, "Installation of two wire collimators in IP5 for Long Range Beam–Beam compensation", EDMS doc. 1705791, LHC–TC–EC–0007, CERN, Geneva, Switzerland (2018).

[48] G. Sterbini *et al.*, "First Results of the Compensation of the Beam-Beam Effect with DC Wires in LHC", Proceedings in the International Particle Accelerator Conference IPAC19, 19th-24th May, Melbourne, Australia.

[49] A. Rossi, Y. Papaphilippou, A. Poet, G. Sterbini, "Moving of Two Wire Collimators for BBLR Compensation from B2 to B1 on IR1 and IR5", LHC-TC-EC-0019, EDMS doc 2054712, CERN, Geneva, Switzerland, Feb 2019.
https://edms.cern.ch/ui/#!master/navigator/document?D:100246831:100246831:approvalAndComments.

[50] R. Bruce and S. Redaelli, "Installation of a primary collimator with orbit pickups (TCPP) replacing a TCP", EDMS doc. 1705737, LHC–TC–EC–0005, CERN, Geneva, Switzerland (2016).

[51] H. Burkhardt, "High-Beta Optics and Running Prospects", Instruments 2019, 3, 22.
https://doi.org/10.3390/instruments3010022.

[52] H. Garcia-Morales *et al.*, "Special Collimation System Configurations for the LHC High-β Runs", 9th International Particle Accelerator Conference IPAC2018, Vancouver, BC, Canada.
http://accelconf.web.cern.ch/AccelConf/ipac2018/papers/mopml012.pdf.

[53] D. Mirarchi, "Crystal Collimation During High-β Runs".
https://indico.cern.ch/event/770857/contributions/3202228/attachments/1751242/2838042/ColWG$_$cry$_$DM.pdf.

[54] A. Mereghetti *et al.*, "Collimation System Upgrades for the High Luminosity Large Hadron Collider and Expected Run-III Cleaning Performance", Proceedings in the International Particle Accelerator Conference IPAC19, 19th-24th May, Melbourne, Australia.

[55] G. Rumolo *et al.*, "What to expect from the injectors during Run 3", in these proceedings, January 2019.

[56] S. R. Klein, "Localized beampipe heating due to e- capture and nuclear excitation in heavy ion colliders", Nucl. Inst. & Methods A, 2001, pag.51, Vol. 459.

[57] J. M. Jowett *et al.*, "Limits to the Performance of the LHC with Ion Beams", Proc. of the European Particle Accelerator Conf. 2004, Lucerne, 2004.

[58] R. Bruce *et al.*, "Beam losses from ultraperipheral nuclear collisions between Pb ions in the Large Hadron Collider and their alleviation", Phys. Rev. ST Accel. Beams, July 2009, 7-071002-12.

[59] M. Schaumann *et al.*, "LHC BFPP Quench Test with Ions (2015)", CERN-ACC-NOTE-2016-0024, 2016. `https://cds.cern.ch/record/2127951?ln=en`.